Silver as an Exopolyhedral Auxiliary to the Rhenacarborane Anion $[Re(CO)_3(\eta^5\text{-}7,8\text{-}C_2B_9H_{11})]^{-}$†

Dianne D. Ellis,‡ John C. Jeffery,# Paul A. Jelliss,‡,§ Jason A. Kautz,‡ and F. Gordon A. Stone*,‡

Department of Chemistry and Biochemistry, Baylor University, Waco, Texas 76798-7348, and The School of Chemistry, The University of Bristol, Bristol BS8 1TS, U.K.

Received October 16, 2000

The rhenacarborane salt $Cs[Re(CO)_3(\eta^5\text{-}7,8\text{-}C_2B_9H_{11})]$ (**1**) has been used to synthesize the tetranuclear metal complex $[\{ReAg(\mu\text{-}10\text{-}H\text{-}\eta^5\text{-}7,8\text{-}C_2B_9H_{10})(CO)_3\}_2\{\mu\text{-}Ph_2P(CH_2)_2PPh_2\}]$ (**3**) where two $[ReAg(\mu\text{-}10\text{-}H\text{-}\eta^5\text{-}7,8\text{-}C_2B_9H_{10})(CO)_3]$ fragments have been shown by X-ray crystallography to be bridged by a single 1,2-bis(diphenylphosphino)ethane ligand. Reaction of **1** with $Ag[BF_4]$ in the presence of the ligands bis- or tris(pyrazol-1-yl)methane yields the complexes $[ReAg(\mu\text{-}10\text{-}H\text{-}\eta^5\text{-}7,8\text{-}C_2B_9H_{10})(CO)_3\{\kappa^2\text{-}CH_2(C_3H_3N_2\text{-}1)_2\}]$ (**4**) or $[\{ReAg(\mu\text{-}10\text{-}H\text{-}\eta^5\text{-}7,8\text{-}C_2B_9H_{10})(CO)_3\}_2\{\mu\text{-}\kappa^1,\kappa^2\text{-}CH(C_3H_3N_2\text{-}1)_3\}]$ (**5**), respectively. From X-ray studies, the former comprises a Re−Ag bond bridged by the carborane cage and with the bis(pyrazol-1-yl)methane coordinating the silver(I) center in an asymmetric κ^2 mode. Complex **5** was unexpectedly found to contain a tris(pyrazol-1-yl)methane bridging two $[ReAg(\mu\text{-}10\text{-}H\text{-}\eta^5\text{-}7,8\text{-}C_2B_9H_{10})(CO)_3]$ fragments in a κ^1,κ^2 manner. Treatment of **1** with $Ag[BF_4]$ in the presence of 2,2′-dipyridyl and 2,2′:6′,2″−terpyridyl yields $[ReAg(\mu\text{-}10\text{-}H\text{-}\eta^5\text{-}7,8\text{-}C_2B_9H_{10})(CO)_3\{\kappa^2\text{-}(C_5H_4N\text{-}2)_2\}]$ (**6**) and $[ReAg(\mu\text{-}10\text{-}H\text{-}\eta^5\text{-}7,8\text{-}C_2B_9H_{10})(CO)_3\{\kappa^3\text{-}C_5H_3N(C_5H_4N\text{-}2)_2\text{-}2,6\}]$ (**7**). The X-ray structure determination of **7** revealed an unusual pentacoordinated silver(I) center, asymmetrically ligated by a κ^3-2,2′:6′,2″-terpyridyl molecule. The same synthetic procedure using *N*,*N*,*N*′,*N*′-tetramethylethylenediamine gave a tetranuclear metal complex $[\{ReAg(\mu\text{-}10\text{-}H\text{-}\eta^5\text{-}7,8\text{-}C_2B_9H_{10})(CO)_3\}_2\{\mu\text{-}Me_2N(CH_2)_2NMe_2\}_2]$ (**8**) which is believed, in the solid state, to be bridged between the silver atoms by two of the diamine molecules. The salt **1** with $Ag[BF_4]$ in the absence of any added ligand gave the tetrameric cluster $[ReAg\{\mu\text{-}5,6,10\text{-}(H)_3\text{-}\eta^5\text{-}7,8\text{-}C_2B_9H_8\}(CO)_3]_4$ (**9**) where, in the solid state, four $[ReAg(\mu\text{-}10\text{-}H\text{-}\eta^5\text{-}7,8\text{-}C_2B_9H_{10})(CO)_3]$ units are held together by long interunit B−H ⇀ Ag bonds.

Introduction

The literature is replete with examples of compounds of silver(I) complexed by phosphine ligands, primarily PPh_3.[1] Another well-established ligand for silver(I) is tris(pyrazol-1-yl)borate and its derivatives,[1a,2] which can, with appropriate modulation of the ligand, render the silver an effective binder of even π-acidic ligands as shown by the elegant work of Dias and co-workers.[2f] The branches of silver(I)-phosphine and silver(I)-tris(pyrazol-1-yl)borate chemistry have been examined in studies by Bruce and Gioia Lobbia and their co-workers.[2b,c,3] Much less studied are related complexes involving bis- and tris(pyrazol-1-yl)methane groups although there are seminal reports by the groups of Gioia Lobbia[4] and Reger,[5] respectively. Silver(I) complexes with 2,2′-dipyridyl and 2,2′:6′,2″-terpyridyl molecules are, on the other hand, ubiquitous, and many such species have been characterized.[1a,6]

We report herein new complexes incorporating AgL (L = $Ph_2P(CH_2)_2PPh_2$, bis- and tris(pyrazol-1-yl)methanes, di- and terpyridyls) moieties as exopolyhedral groups in complexes formed by the rhenacarborane anion derived from the salt $Cs[Re(CO)_3(\eta^5\text{-}7,8\text{-}C_2B_9H_{11})]$ (**1**). Silver(I) carborane complexes are themselves rare,[7] though we have recently described the binding of $[Ag(PPh_3)]^+$ fragments exopolyhedrally to $[Re(CO)_3$-

* To whom correspondence should be addressed.

† The compounds described in this paper have a rhenium atom incorporated into a *closo*-1,2-dicarba-3-rhenadodecaborane structure. However, to avoid a complicated nomenclature for the complexes reported, and to relate them to the many known rhenium species with η-coordinated cyclopentadienyl ligands, we treat the cages as *nido*-11-vertex ligands with numbering as for an icosahedron from which the twelfth vertex has been removed.

‡ Baylor University.

The University of Bristol.

§ Current address: Department of Chemistry, Saint Louis University, St. Louis, MO 63103.

(1) (a) Lancashire, R. J. In *Comprehensive Coordination Chemistry*; Wilkinson, G., Gillard, R. D., McCleverty, J. A., Eds.; Pergamon Press: Oxford, U.K., 1987; Vol. 5, pp 775−838. (b) Bachman, R. E.; Andretta, D. F. *Inorg. Chem.* **1998**, *37*, 5657 and references therein.

(2) (a) Trofimenko, S. *Chem. Rev.* **1993**, *93*, 943. (b) Abu Salah, O. M.; Ashby, G. S.; Bruce, M. I.; Pederzolli, E. A.; Walsh, J. D. *Aust. J. Chem.* **1979**, *32*, 1613. (c) Bruce, M. I.; Walsh, J. D. *Aust. J. Chem.* **1979**, *32*, 2753. (d) Dias, H. V. R.; Lu, H.-L.; Ratcliff, R. E.; Bott, S. G. *Inorg. Chem.* **1995**, *34*, 1975. (e) Dias, H. V. R.; Jin, W.; Kim, H.-J.; Lu, H.-L. *Inorg. Chem.* **1996**, *35*, 2317. (f) Dias, H. V. R.; Wang, Z.; Jin, W. *Inorg. Chem.* **1997**, *36*, 6205.

(3) Calogero, S.; Gioia Lobbia, G.; Pellei, M.; Pettinari, C.; Santini, C.; Valle, G. *Inorg. Chem.* **1998**, *37*, 890.

(4) (a) Lorenzotti, A.; Bonati, F.; Cingolani, A.; Gioia Lobbia, G.; Leonesi, D.; Bovio, B. *Inorg. Chim. Acta* **1990**, *170*, 199. (b) Gioia Lobbia, G.; Bonati, F.; Cingolani, A.; Leonesi, D. *Synth. React. Inorg. Met.-Org. Chem.* **1989**, *19*, 827.

(5) Collins, J. E.; Liable-Sands, L. M.; Reger, D. L.; Rheingold, A. L.; Yap, G. P. A. *Organometallics* **1997**, *16*, 349.

(6) McWhinnie, W. R.; Miller, J. D. *Adv. Inorg. Chem. Radiochem.* **1969**, *12*, 135.

(7) (a) Colquhoun, H. M.; Greenhough, T. J.; Wallbridge, M. G. H. *J. Chem. Soc., Dalton Trans.* **1980**, 192. (b) Shelly, K.; Finster, D. C.; Lee, Y. J.; Scheidt, W. R.; Reed, C. A. *J. Am. Chem. Soc.* **1985**, *107*, 5955. (c) Eigenbrot, C. W.; Liston, D. J.; Reed, C. A.; Scheidt, W. R. *Inorg. Chem.* **1987**, *26*, 2739. (d) Park, Y.-W.; Kim, J.; Do, Y. *Inorg. Chem.* **1994**, *33*, 1. (e) Patmore, N. J.; Steed, J. W.; Weller, A. S. *J. Chem. Soc., Chem. Commun.* **2000**, 1055.

10.1021/ic001140c CCC: $20.00
Published on Web 03/17/2001

Chart 1

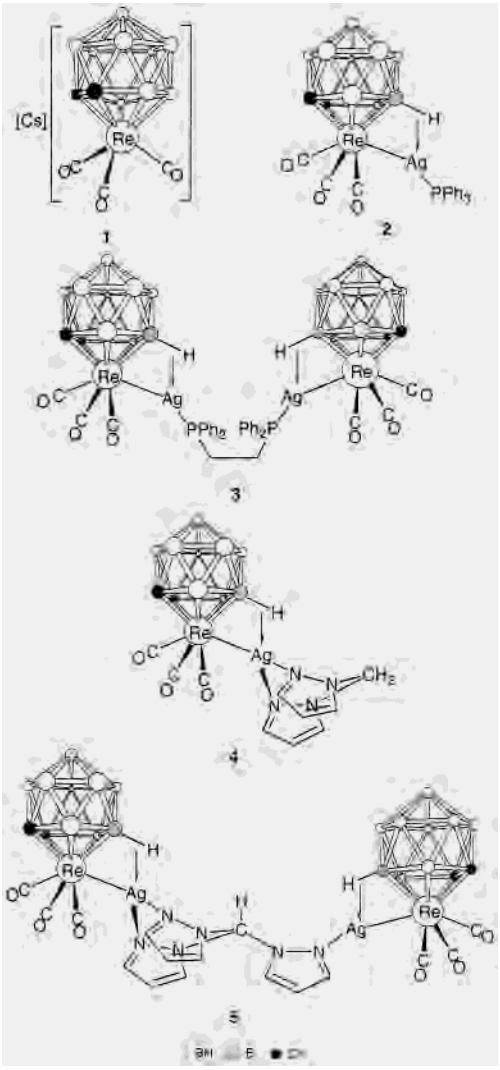

$(\eta^5\text{-}7,8\text{-}C_2B_9H_{11})]^-$ and $[M(CO)_x(L)(\eta^5\text{-}7\text{-}CB_{10}H_{11})]^-$ (M = Fe, $x = 2$, L = CO; M = Mo, $x = 3$, L = PPh_3) anions via one or two B−H ⇀ Ag 3-center-2-electron bonds.[8] The first species has a direct Re−Ag bond in the solid state, while the last two do not contain Fe−Ag or Mo−Ag connectivities, thus adding to a growing class of *exo*−*closo* dimetallacarboranes with no M−M bonds. The discussion will be concluded by the description of the surprising and unexpected structure of a tetrameric $(ReAg)_4$ complex formed between $[Re(CO)_3(\eta^5\text{-}7,8\text{-}C_2B_9H_{11})]^-$ and naked Ag^+ cations bearing no ancillary ligands. The NMR data for the new complexes are presented but the structures of many of these new species could only be firmly established by X-ray diffraction studies because of the tendency of the *exo*-AgL fragments to undergo facile dynamic activity in solution.

Results and Discussion

The structural architecture of the recently reported complex $[ReAg(\mu\text{-}10\text{-}H\text{-}\eta^5\text{-}7,8\text{-}C_2B_9H_{10})(CO)_3(PPh_3)]$ (**2**)[8a] is perhaps unremarkable when compared with the structures of several other molecules where a $[closo\text{-}3,1,2\text{-}MC_2B_9]^-$ or $[closo\text{-}2,1\text{-}MCB_{10}]^-$ metallacarborane is bound exopolyhedrally by a $[M'(PPh_3)]^+$ (M′ = Cu, Ag, Au) moiety via an M−M′ bond bridged by a B−H ⇀ M′ system.[9,10] Nevertheless **2** is a significant addition to the very limited number of structurally characterized complexes with Re−Ag bonds.[11] Complex **2** is particularly noteworthy in that in solution the *exo*-$[Ag(PPh_3)]^+$ group readily detaches from the rhenium vertex of the *closo*-3,1,2-$ReC_2B_9H_{11}$ ensemble and effectively scrambles about the polyhedral cage surface, a dynamic feature which cannot be frozen out down to −80 °C. Intermediate species can be envisaged which bear resemblance to the *exo*−*closo* complexes $[M(CO)_x(L)\{\mu\text{-}5,9\text{-}(H)_2\text{-}5,9\text{-}Ag(PPh_3)\text{-}\eta^5\text{-}7\text{-}CB_{10}H_9\}]$ (M = Fe, $x = 2$, L = CO; M = Mo, $x = 3$, L = PPh_3) where an *exo*-$[Ag(PPh_3)]^+$ unit is bound to the $[closo\text{-}2,1\text{-}MCB_{10}H_{11}]^-$ cages via two B−H ⇀ Ag bonds.[8b] However, the reader should note the subtle difference in the constituent carborane cages (CB_{10} versus C_2B_9) between the Fe and Mo species and complex **2**. To investigate further this rhenium−silver system we considered that substituting $Ph_2P(CH_2)_2PPh_2$ for PPh_3 on Ag^+ might do one of two things: (i) the Re−Ag and B−H ⇀ Ag bonds could be retained and the $Ph_2P(CH_2)_2PPh_2$ ligand would bridge two Re−Ag fragments or (ii) the $Ph_2P(CH_2)_2PPh_2$ ligand, as it is apt to do, would chelate a single silver center and disrupt the Re−Ag and/or β-B−H ⇀ Ag bonding in some way, possibly displacing the silver atom to give an *exo*−*closo* complex with no direct Re−Ag linkage.

Complex **1** was treated with a 1:1 mixture of $Ag[BF_4]$ and $Ph_2P(CH_2)_2PPh_2$ in THF. A single product $[\{ReAg(\mu\text{-}10\text{-}H\text{-}\eta^5\text{-}7,8\text{-}C_2B_9H_{10})(CO)_3\}_2\{\mu\text{-}Ph_2P(CH_2)_2PPh_2\}]$ (**3**) was isolated in moderate yield. The IR spectrum in the CO region (2024, 1945, and 1920 cm^{-1}, Table 1) is nearly identical with that for **2** (2024, 1943, and 1924 cm^{-1}). The ^1H NMR spectrum (Table 2) confirms that the ratio of carborane cage to $Ph_2P(CH_2)_2PPh_2$ is 2:1 by virtue of the relative integrals of the signals due to the cage CH protons (δ 3.35, 2 H) and the phenyl groups of the phosphine ligand (δ 7.27−7.56, 20 H) and methylene protons (δ 2.61, 4 H). This strongly suggests that the $Ph_2P(CH_2)_2PPh_2$ molecule adopts the bridging mode mentioned in (i) (vide supra). Complex **3** is highly dynamic in solution and this property is maintained even at low temperatures (−80 °C), despite the increased molecular bulk. As with **2** the dynamic behavior probably involves scrambling of the Ag^+ centers over the cage surface. For this reason the ^1H and $^{11}B\{^1H\}$ NMR spectra of **3** do not display any interesting features such as those frequently encountered with agostic B−H ⇀ M bonding.[12] Moreover, in the $^{13}C\{^1H\}$ NMR spectrum only one CO resonance is seen, also in accord with dynamic behavior. In the room temperature $^{31}P\{^1H\}$ NMR spectrum only a broad doublet centered at δ 18.7 ($J(AgP)$ = ca. 633 Hz) is observed, suggesting perhaps that the phosphine is undergoing very limited exchange between the silver atoms. The same spectrum measured at −60 °C showed a more resolved concentric pair of doublet-of-doublets with

(8) (a) Ellis, D. D.; Jelliss, P. A.; Stone, F. G. A. *Organometallics* **1999**, *18*, 4982. (b) Ellis, D. D.; Franken, A.; Jelliss, P. A.; Kautz, J. A.; Stone, F. G. A.; Yu, P.-Y. *J. Chem. Soc., Dalton Trans*. **2000**, 2509.

(9) (a) Do, Y.; Knobler, C. B.; Hawthorne, M. F. *J. Am. Chem. Soc.* **1987**, *109*, 1853. (b) Kang, H. C.; Do, Y.; Knobler, C. B.; Hawthorne, M. F. *Inorg. Chem.* **1988**, *27*, 1716.

(10) (a) Batten, S. A.; Jeffery, J. C.; Jones, P. L.; Mullica, D. F.; Rudd, M. D.; Sappenfield, E. L.; Stone, F. G. A.; Wolf, A. *Inorg. Chem*. **1997**, *36*, 2570. (b) Cabioch, J.-L.; Dossett, S. J.; Hart, I. J.; Pilotti, M. U.; Stone, F. G. A. *J. Chem. Soc., Dalton Trans.* **1991**, 519. (c) Jeffery, J. C.; Stone, F. G. A.; Topalooğlu, I. *J. Organomet. Chem.* **1993**, *451*, 205. (d) Ellis, D. D.; Couchman, S. M.; Jeffery, J. C.; Malget, J. M.; Stone, F. G. A. *Inorg. Chem.* **1999**, *38*, 2981. (e) Ellis, D. D.; Franken, A.; Stone, F. G. A. *Organometallics* **1999**, *18*, 2362.

(11) (a) Beringhelli, T.; Ciani, G.; D'Alfonso, G.; Freni, M.; Sironi, A. *J. Organomet. Chem*. **1985**, *295*, C7. (b) Connelly, N. G.; Howard, J. A. K.; Spencer, J. L.; Woodley, P. K. *J. Chem. Soc., Dalton Trans.* **1984**, 2003.

(12) Brew, S. A.; Stone, F. G. A. *Adv. Organomet. Chem.* **1993**, *35*, 135.

Table 1. Analytical and Physical Data

compound[a]	yield (%)	ν_{max}(CO)[b] (cm^{-1})	analysis (%)[c] C	H	N
[{ReAg(μ-10-H-η^5-7,8-$C_2B_9H_{10}$)$(CO)_3$}$_2${μ-$Ph_2P(CH_2)_2PPh_2$}] (**3**)	57	2024vs, 1945s, 1920s	32.3 (30.5)	3.8 (3.3)[d]	
[ReAg(μ-10-H-η^5-7,8-$C_2B_9H_{10}$)$(CO)_3${κ^2-$CH_2(C_3H_3N_2-1)_2$}] (**4**)	67	2022vs, 1952s, 1933s	22.1 (21.9)	3.0 (2.9)	8.4 (8.5)
[{ReAg(μ-10-H-η^5-7,8-$C_2B_9H_{10}$)$(CO)_3$}$_2${μ-κ^1,κ^2-$CH(C_3H_3N_2$-1)$_3$}] (**5**)	73	2020vs, 1936s, 1918s	21.5 (21.1)	4.4 (4.3)	4.5 (4.5)
[ReAg(μ-10-H-η^5-7,8-$C_2B_9H_{10}$)$(CO)_3${κ^2-(C_5H_4N-2)$_2$}] (**6**)[e]	80	2018vs, 1933s, 1917s	27.2 (27.0)	2.8 (2.9)	4.2 (4.2)
[ReAg(μ-10-H-η^5-7,8-$C_2B_9H_{10}$)$(CO)_3${κ^3-C_5H_3N(C_5H_4N-2)$_2$-2,6}] (**7**)[e]	86	2016vs, 1919vs br	31.7 (32.3)	2.8 (3.0)	5.5 (5.7)
[{ReAg(μ-10-H-η^5-7,8-$C_2B_9H_{10}$)$(CO)_3$}$_2${μ-$Me_2N(CH_2)_2NMe_2$}$_2$] (**8**)[e]	31	2018vs, 1934s, 1916s	19.5 (19.5)	2.6 (2.6)	6.6 (6.8)
[ReAg{μ-5,6,10-$(H)_3$-η^5-7,8-$C_2B_9H_8$}$(CO)_3$]$_4$ (**9**)	73	2026vs, 1942s, 1929s	11.8 (11.8)	2.2 (2.2)	

[a] All compounds are white or off-white. [b] Measured in CH_2Cl_2; medium-intensity broad bands observed at ca. 2550 cm^{-1} in the spectra of all the compounds are due to B−H absorptions. [c] Calculated values are given in parentheses. [d] Microanalysis consistently found to be 1.8% too high for carbon. FAB mass spectra: positive ion, *m*/*z* 1018.2 [**3** − Re$(CO)_3$(η^5-7,8-$C_2B_9H_{11}$)]$^+$ (calcd 1016.8), negative ion, *m*/*z* 403.7 [Re$(CO)_3$(η^5-7,8-$C_2B_9H_{11}$)]$^-$ (calcd 402.7). [e] Light sensitive compound, turns brown.

Table 2. Hydrogen-1, Carbon-13, and Boron-11 NMR Data[a]

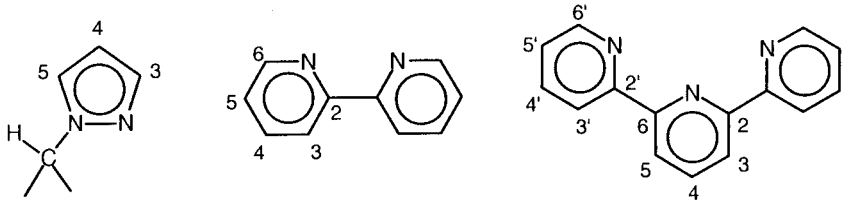

compd	^{1}H/δ [b]	^{13}C/δ [c]	^{11}B/δ [d]
3[e]	7.56−7.27 (m, 20 H, Ph), 3.35 (s br, 4 H, cage CH), 2.61 (s, 4 H, CH_2)	192.0 (CO), 133.4−128.6 (Ph), 36.4 (br, cage CH), 24.4 (AXX′, CH_2, $N = 30$[f])	−1.3 (1 B), −9.9 (2 B), −15.2 (2 B), −18.3 (2 B), −22.1 (2 B)
4	7.78, 7.77 (d × 2, 4 H, $H^{3,5}$, J(HH) = 2, 2), 6.45 (dd, 2 H, H^4, J(HH) = 2, 2), 6.34 (s, 2 H, CH_2), 3.29 (s br, 2 H, cage CH)	192.9 (CO), 144.0, 131.8, 108.0 (NC_3H_3), 64.7 (CH_2), 35.2 (br, cage CH)	−2.4 (1 B), −10.2 (2 B), −14.9 (2 B), −18.2 (1 B), −20.7 (1 B), −22.9 (2 B)
5	8.27 (s, 1 H, CH), 7.94, 7.85 (d × 2, 6 H, $H^{3,5}$, J(HH) = 2, 2), 6.60 (dd, 3 H, H^4, J(HH) = 2, 2), 3.29 (s br, 4 H, cage CH)	192.4 (CO), 145.7, 133.1, 109.1 (NC_3H_3), 81.1 (CH), 35.8 (br, cage CH)	−1.9 (1 B), −10.2 (2 B), −15.2 (2 B), −17.9 (1 B), −21.6 (1 B), −22.8 (2 B)
6	8.75 (dd, 2 H, H^2, J(HH) = 1, 5), 8.19 (d, 2 H, H^5, J(HH) = 8), 8.05 (ddd, 2 H, H^4, J(HH) = 1, 8, 8), 7.58 (dd, 2 H, H^3, J(HH) = 5, 8), 3.29 (s br, 2 H, cage CH)	192.7 (CO), 151.8 (C^2), 151.4 (C^6), 139.7, 126.2, 122.6 ($C^{3,4,5}$), 35.2 (br, cage CH)	−2.5 (1 B), −10.2 (2 B), −15.0 (2 B), −18.1 (1 B), −20.1 (1 B), −22.9 (2 B)
7	8.48 (m, 2 H, $H^{3,5}$), 8.19−7.96 (m, 7 H, H^4, $H^{3',4',6'}$), 7.50−7.45 (m, 2 H, $H^{5'}$), 3.08 (s br, 2 H, cage CH)	193.14 (CO), 153.5, 152.2 ($C^{2,6}$, $C^{2'}$), 151.7 ($C^{6'}$), 140.8, 139.5, 126.0, 123.7, 123.4 ($C^{3-5,3'-5'}$), 34.5 (br, cage CH)	−3.1 (1 B), −10.4 (2 B), −14.8 (2 B), −18.0 (1 B), −19.9 (1 B), −23.5 (2 B)
8	3.20 (s br, 2 H, cage CH), 2.60 (s, 4 H, CH_2), 2.54 (s, 12 H, Me)	193.0 (CO), 58.4 (CH_2), 48.6 (Me), 34.9 (br, cage CH)	−2.9 (1 B), −10.3 (2 B), −15.4 (2 B), −18.8 (1 B), −20.0 (1 B), −22.9 (2 B)
9[g]	3.31 (s br, 2 H, cage CH)	191.1 (CO), 36.1 (br, cage CH)	−1.7 (1 B), −10.9 (2 B), −15.2 (2 B), −17.5 (1 B), −22.6 (3 B)

[a] Chemical shifts (δ) in ppm, coupling constants (J) in Hz, measurements in CD_2Cl_2, and at room temperature. [b] Resonances for terminal BH protons occur as broad unresolved signals in the range δ ca. −2 to 3. [c] Hydrogen-1 decoupled, chemical shifts are positive to high frequency of $SiMe_4$. [d] Hydrogen-1 decoupled, chemical shifts are positive to high frequency of BF_3·Et_2O (external). All resonances are broad, with some signals corresponding to overlapping peaks which do not necessarily indicate symmetry equivalence. [e] ^{31}P{^{1}H} NMR (−60 °C): δ −19.9 [dd × 2, $^1J(^{109}AgP)$ = 678, $^1J(^{107}AgP)$ = 603, $^4J(^{109}AgP)$ = 58, $^4J(^{107}AgP)$ = 14]. [f] Insufficient resolution prevents full analysis of coupling constants; $N = |J(AX) + J(AX')|$. [g] Measured in CD_2Cl_2 with a small amount of added THF.

typical ^{109}Ag−^{31}P and ^{107}Ag−^{31}P one-bond couplings of 678 and 603 Hz, respectively.[13]

To confirm the bridging nature of the $Ph_2P(CH_2)_2PPh_2$ ligand in **3**, single crystals were grown and an X-ray diffraction study carried out. The salient bond lengths and angles are given in Table 3, and the structure is shown in Figure 1. The CH_2CH_2 fragment of the phosphine straddles a crystallographic center of symmetry, resulting in duplicate bond distances in each half of the molecule. The Ag−P bond (2.3912(14) Å) is within the accepted range[14] and the Re−Ag connectivity is clearly that of a single bond (2.9457(6) Å) being similar to that in complex **2** (2.9344(12) Å).[8a] The β-B−H ⇀ Ag agostic group in complex **3** (B(4)−Ag = 2.442(6) Å) can be identified on both ends of the molecule, so that the local environment about the silver atoms is essentially similar to that in complex **2**, although the B(4)−Ag−P angle in the former (157.2(2)°) is marginally more acute than that in the latter (171.1(3)°). This is probably due to a response in complex **3** preventing the *endo*-Re$(CO)_3$ vertex

(13) Muetterties, E. L.; Alegranti, C. W. *J. Am. Chem. Soc.* **1972**, *94*, 6386.

(14) Allen, F. H.; Brammer, L.; Kennard, O.; Orpen, A. G.; Taylor, R.; Watson, D. G. *J. Chem. Soc., Dalton Trans.* **1989**, S1.

Table 3. Selected Internuclear Distances (Å) and Angles (deg) for [{ReAg(μ-10-H-η^5-7,8-$C_2B_9H_{10}$)$(CO)_3$}$_2${μ-$Ph_2P(CH_2)_2PPh_2$}] (**3**)

Re−C(5)	1.923(6)	Re−C(4)	1.925(7)	Re−C(3)	1.931(6)	Re−C(1)	2.292(5)
Re−C(2)	2.313(6)	Re−B(5)	2.341(6)	Re−B(3)	2.367(6)	Re−B(4)	2.405(6)
Re−Ag	2.9457(6)	C(3)−O(3)	1.143(6)	C(4)−O(4)	1.152(7)	C(5)−O(5)	1.165(7)
B(4)−Ag	2.442(6)	Ag−H(4)	1.96(5)	Ag−P	2.3912(14)	Ag−H(10a)[a]	2.45(5)
Ag−B(10a)[a]	3.490(9)						

C(5)−Re−C(4)	92.6(2)	C(5)−Re−C(3)	84.6(2)	C(4)−Re−C(3)	85.8(2)
O(3)−C(3)−Re	178.1(5)	O(4)−C(4)−Re	177.2(5)	O(5)−C(5)−Re	177.3(5)
H(4)−Ag−P	146(2)	P−Ag−B(4)	157.2(2)	P−Ag−Re	129.93(4)

[a] Symmetry transformations used to generate equivalent atoms: $-x, y, -z + {}^1/_2$.

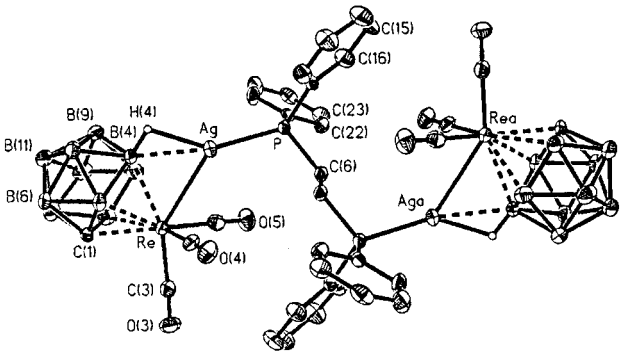

Figure 1. Structure of [{ReAg(μ-10-H-η^5-7,8-$C_2B_9H_{10}$)$(CO)_3$}$_2${μ-$Ph_2P(CH_2)_2PPh_2$}] (**3**), showing the crystallographic labeling scheme. Thermal ellipsoids are shown at the 40% probability level. Only the agostic hydrogen atoms are shown for clarity.

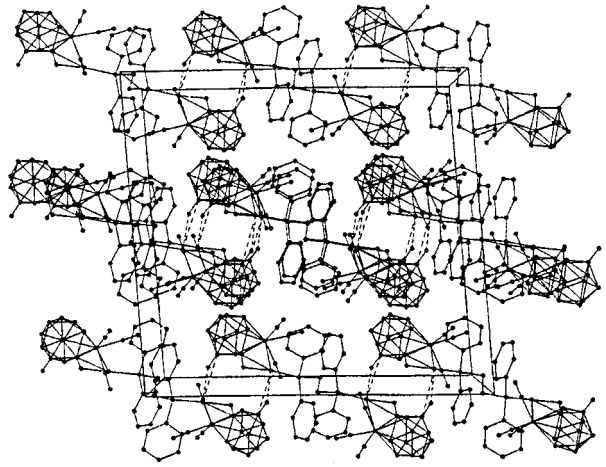

Figure 2. Molecular packing diagram of **3** viewed down the crystallographic *b* axis. Intermolecular B−H···Ag interactions are shown by the dotted lines.

from approaching the distal phenyl groups too closely. The Re−Ag−P angles are closer in magnitude for both molecules (129.93(4) (**3**) and 134.74(8) (**2**)). A long intermolecular B−H···Ag interaction (Ag···B(10a) = 3.490(9) Å) is also apparent and can be seen in the packing diagram represented in Figure 2. This involves the B(10a)−H(10a) bond from the noncoordinating B_5 belt of an adjacent molecule interacting with the silver atom. Symmetry requirements result in two of these interactions per pair of molecules. Such intermolecular bonding was observed in the crystal structure of [$Mo(CO)_3(PPh_3)$-{μ-5,9-$(H)_2$-5,9-Ag(PPh_3)-η^5-7-$CB_{10}H_9$}] and accredited to long-range electrostatic forces between isolated pairs of molecules.[8b] A facet of this phenomenon in **3**, however, is that the molecules are held together, albeit weakly, in chains along the crystallographic *c* axis (Figure 2).

The failure of the $Ph_2P(CH_2)_2PPh_2$ ligand to chelate a single silver center initiated a search for more suitable ligands for this purpose. The propensity for the pyrazolyl type ligands to behave in this way and their well-established complexation with silver(I) centers provided an obvious route. Thus a neutral complex [ReAg(μ-10-H-η^5-7,8-$C_2B_9H_{10}$)$(CO)_3${κ^2-$CH_2(C_3H_3N_2$-1)$_2$}] (**4**) was isolated when salt **1** was treated with a 1:1 mixture of Ag[BF_4] and $CH_2(C_3H_3N_2$-1)$_2$ (bis(pyrazol-1-yl)methane). Peak integrals in the ^{1}H NMR spectrum (Table 2) confirm a 1:1:1 adduct formation between the anion of salt **1**, an Ag^+ cation, and a molecule of $CH_2(C_3H_3N_2$-1)$_2$. The signals in this spectrum for the pyrazolyl protons (d × 2 at δ 7.78 and 7.77 (J(HH) = 2 and 2 Hz), dd at δ 6.45 (J(HH) = 2 and 2 Hz)) indicate that both rings are equivalent in solution as does the observation of three peaks in the ^{13}C{^{1}H} NMR spectrum at δ 144.0, 131.8, and 108.0. The presence of the methylene bridge is verified by resonances in the ^{1}H and ^{13}C{^{1}H} NMR spectra at δ 6.34 and 64.7, respectively. However, the observation of only one signal in the ^{1}H NMR for the CH_2 group, one peak (δ 192.9) in the ^{13}C{^{1}H} spectrum for the Re−CO carbonyl carbon nuclei, and no spectral features due to a B−H ⇀ Ag system in the ^{1}H or ^{11}B{^{1}H} spectra lead us to conclude that complex **4** is highly dynamic in solution.

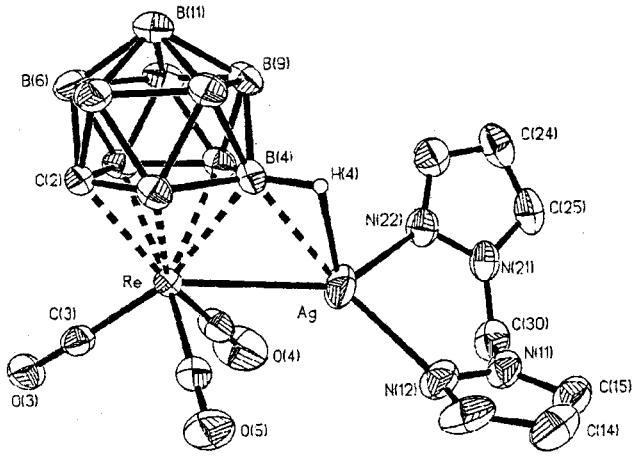

Figure 3. Structure of [ReAg(μ-10-H-η^5-7,8-$C_2B_9H_{10}$)$(CO)_3${κ^2-CH_2-$(C_3H_3N_2$-1)$_2$}] (**4**), showing the crystallographic labeling scheme. Thermal ellipsoids are shown at the 40% probability level. Only the agostic hydrogen atom is shown for clarity.

Recourse to a single-crystal X-ray study was necessary and therefore undertaken. The structure of complex **4** is shown in Figure 3 and selected internuclear distances and angles are given in Table 4. The Re−Ag bond (2.8825(7) Å) is marginally shorter than that observed in complex **3** (2.9457(6) Å), and the β-B−H ⇀ Ag bonding, while still perceptible, is slightly weaker than in **3** with the Ag−B(4) distance a little longer (2.507(6) Å) than the corresponding distance in **3** (2.442(6) Å). These small structural discrepancies are no doubt due to the change in the nature of the ligation at the silver center. The bis(pyrazol-1-yl)methane ligand chelates the silver atom in a κ^2 manner as had been expected, but not in a symmetric fashion with respect to the plane encompassing the Re, Ag, and B(4) atoms. The

Table 4. Selected Internuclear Distances (Å) and Angles (deg) for [ReAg(μ-10-H-η^5-7,8-$C_2B_9H_{10}$)(CO)$_3$\{κ^2-$CH_2(C_3H_3N_2$-1)$_2$\}] (**4**)

Re−C(4)	1.906(5)	Re−C(5)	1.922(5)	Re−C(3)	1.925(5)	Re−C(1)	2.294(5)
Re−C(2)	2.305(4)	Re−B(5)	2.345(5)	Re−B(3)	2.366(5)	Re−B(4)	2.401(5)
Re−Ag	2.8825(7)	B(4)−Ag	2.507(6)	C(3)−O(3)	1.148(6)	C(4)−O(4)	1.147(7)
C(5)−O(5)	1.142(6)	Ag−H(4)	2.07(5)	Ag−N(12)	2.279(5)	Ag−N(22)	2.347(4)

C(4)−Re−C(5)	94.8(2)	C(4)−Re−C(3)	83.4(2)	C(5)−Re−C(3)	88.9(2)
C(4)−Re−B(4)	112.4(2)	C(5)−Re−B(4)	98.5(2)	C(3)−Re−B(4)	161.7(2)
C(4)−Re−Ag	65.8(2)	C(5)−Re−Ag	73.9(2)	C(3)−Re−Ag	142.53(14)
B(4)−Re−Ag	55.75(13)	Re−B(4)−Ag	71.9(2)	O(3)−C(3)−Re	177.3(5)
O(4)−C(4)−Re	177.2(6)	O(5)−C(5)−Re	175.5(5)	H(4)−Ag−N(12)	123(2)
H(4)−Ag−N(22)	98(2)	N(12)−Ag−N(22)	86.8(2)	N(12)−Ag−B(4)	146.1(2)
N(22)−Ag−B(4)	107.8(2)	H(4)−Ag−Re	78(2)	N(12)−Ag−Re	137.06(13)
N(22)−Ag−Re	130.24(12)	B(4)−Ag−Re	52.34(12)		

Table 5. Selected Internuclear Distances (Å) and Angles (deg) for [{ReAg(μ-10-H-η^5-7,8-$C_2B_9H_{10}$)(CO)$_3$}$_2$\{μ-κ^1,κ^2-$CH(C_3H_3N_2$-1)$_3$\}] (**5**)

Re(1)−C(12)	1.915(6)	Re(1)−C(11)	1.928(6)	Re(1)−C(13)	1.930(6)	Re(1)−Ag(1)	2.8544(5)
Ag(1)−H(104)	1.88(4)	Ag(1)−N(42)	2.283(4)	Ag(1)−N(32)	2.387(4)	Ag(1)−B(104)	2.509(5)
C(11)−O(11)	1.143(7)	C(12)−O(12)	1.164(7)	C(13)−O(13)	1.147(7)	Re(2)−C(23)	1.930(5)
Re(2)−C(22)	1.930(4)	Re(2)−C(21)	1.937(5)	Re(2)−Ag(2)	2.9286(5)	Ag(2)−H(204)	1.82(4)
Ag(2)−N(52)	2.229(4)	Ag(2)−B(204)	2.452(5)	C(21)−O(21)	1.141(6)	C(22)−O(22)	1.148(6)
C(23)−O(23)	1.146(6)	N(31)−N(32)	1.363(6)	N(41)−N(42)	1.365(5)	N(51)−N(52)	1.357(5)

C(12)−Re(1)−C(11)	85.9(3)	C(12)−Re(1)−C(13)	93.2(2)	C(11)−Re(1)−C(13)	86.0(3)
C(12)−Re(1)−Ag(1)	68.8(2)	C(11)−Re(1)−Ag(1)	142.9(2)	C(13)−Re(1)−Ag(1)	69.6(2)
N(42)−Ag(1)−N(32)	77.96(13)	N(42)−Ag(1)−B(104)	141.0(2)	N(32)−Ag(1)−B(104)	125.3(2)
N(42)−Ag(1)−Re(1)	143.01(9)	N(32)−Ag(1)−Re(1)	125.49(10)	B(104)−Ag(1)−Re(1)	52.93(11)
O(11)−C(11)−Re(1)	178.8(7)	O(12)−C(12)−Re(1)	175.5(5)	O(13)−C(13)−Re(1)	177.4(5)
C(23)−Re(2)−C(22)	93.1(2)	C(23)−Re(2)−C(21)	85.1(2)	C(22)−Re(2)−C(21)	85.8(2)
C(23)−Re(2)−Ag(2)	68.0(2)	C(22)−Re(2)−Ag(2)	72.52(14)	C(21)−Re(2)−Ag(2)	143.85(14)
N(52)−Ag(2)−B(204)	152.4(2)	N(52)−Ag(2)−Re(2)	122.69(10)	B(204)−Ag(2)−Re(2)	52.55(11)
O(21)−C(21)−Re(2)	177.2(5)	O(22)−C(22)−Re(2)	176.1(4)	O(23)−C(23)−Re(2)	175.5(4)

coordinated nitrogen of one pyrazolyl ring (Ag−N(12) = 2.279(5) Å) lies transoid to the B(4) vertex (B(4)−Ag−N(12) 146.1(2)°) and displaced above the Re−Ag−B(4) plane by ca. 1.1 Å as it is viewed in Figure 3. The other pyrazolyl ring is coordinated to the silver by a longer Ag−N(22) bond (2.347(4) Å) and is cisoid to the cage B(4) vertex (B(4)−Ag−N(22) 107.8(2) °), the nitrogen N(22) deviating below the Re−Ag−B(4) plane by ca. 1.8 Å. The Ag−N bond lengths in complex **3** are comparable with those observed in the complex [Ag{κ^2-$CMe_2(C_3H_3N_2$-1)$_2$}][ClO_4] (Ag−N av. 2.323 Å).[4a] The methylene carbon C(30) is also located below the Re−Ag−B(4) plane by ca. 1.0 Å. Whether this significant degree of asymmetry is representative of the orbital requirements about the silver or is a consequence of crystal packing forces or both is a matter for surmise. Detailed calculations on this and related systems in this paper are as yet unavailable.

A similar synthetic procedure to that which gave **4** but using $CH(C_3H_3N_2$-1)$_3$ (tris(pyrazol-1-yl)methane) as a ligand yielded the compound [{ReAg(μ-10-H-η^5-7,8-$C_2B_9H_{10}$)(CO)$_3$}$_2$\{μ-κ^1,κ^2-$CH(C_3H_3N_2$-1)$_3$\}] (**5**) when the reactants **1**, Ag[BF_4], and $CH(C_3H_3N_2$-1)$_3$ were combined in a 2:2:1 ratio. Acknowledging the potential for tris(pyrazol-1-yl)methane ligands to engage in κ^2 or κ^3 ligation, it was expected that if the Re−β-B−H⇀Ag core structure was maintained, at least in the solid state if not in solution, then the $CH(C_3H_3N_2$-1)$_3$ ligand in complex **5** would probably bind in a κ^2 fashion leaving a pendant pyrazolyl ring. Quite unexpectedly this ligand was found in an X-ray structure determination to bridge between two [ReAg(μ-10-H-η^5-7,8-$C_2B_9H_{10}$)(CO)$_3$] fragments in an asymmetric κ^1,κ^2 mode (Table 5 and Figure 4). The rhenium−silver bonds (Re(1)−Ag(1) 2.8544(5) and Re(2)−Ag(2) 2.9286(5) Å) are bridged in the usual β manner by μ-10-H-η^5-7,8-$C_2B_9H_{10}$ carborane cages (Ag(1)−B(104) 2.509(5) and Ag(2)−B(204) 2.452(5) Å). Two of the pyrazolyl rings are coordinated to one silver atom (Ag(1)−N(32) 2.387(4) and Ag(1)−N(42) 2.283(4) Å) so that Ag(1) shares a similar local coordination geometry to the Ag center in complex **4**. The nitrogen atoms N(32) and N(42) are displaced ca. 1.8 and 1.1 Å from either side of the Re(1)−Ag(1)−B(104) mean plane, respectively. The remaining pyrazolyl ring is coordinated to the second silver atom (Ag(2)−N(52) 2.229(4) Å), the ring nitrogen donor being necessarily twisted away from Ag(1). The coordinated nitrogen N(52) is distinctly transoid to the β-boron involved in the B(204)−H(204) ⇀ Ag(2) group (B(204)−Ag(2)−N(52) 152.4(2)°). The nitrogen N(52) also deviates from its associated Re(2)−Ag(2)−B(204) plane by ca. 1.0 Å. Such κ^1,κ^2 bridging is unprecedented for tris(pyrazol-1-yl)methane ligands but has been previously documented for tris(pyrazol-1-yl)borato anions in the structure determinations of the complexes [{CuCl}$_2$\{Cu(η^2-C_2H_4)\}$_2$\{μ-κ^1,κ^2-$BH(C_3H_3N_2$-

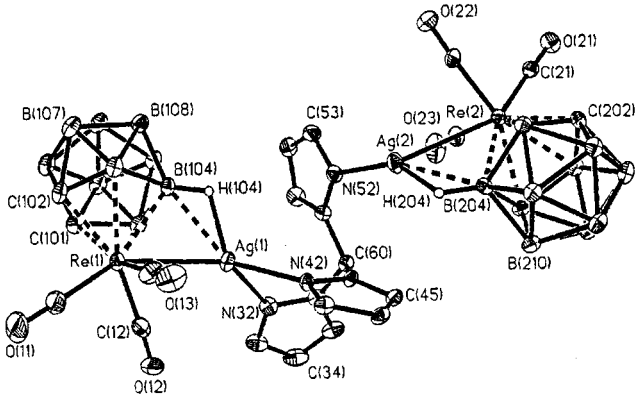

Figure 4. Structure of [{ReAg(μ-10-H-η^5-7,8-$C_2B_9H_{10}$)(CO)$_3$}$_2$\{μ-κ^1,κ^2-$CH(C_3H_3N_2$-1)$_3$\}] (**5**), showing the crystallographic labeling scheme. Thermal ellipsoids are shown at the 40% probability level. Only the agostic hydrogen atoms are shown for clarity.

1)$_3$}$_2$], [Cu{μ-κ^1,κ^2-BH(C$_3$H$_3$N$_2$-1)$_3$}]$_2$, and [Mo{μ-κ^1,κ^2-BH(C$_3$H$_3$N$_2$-1)$_3$}$_2$Cl$_2$].[15] The borato class of ligand has also been shown to κ^1,κ^1,κ^1 triply bridge a set of three silver atoms in the complex [Ag$_3$(μ_3-κ^1,κ^1,κ^1-BH{C$_3$H$_2$N$_2$(C$_6$H$_5$OMe-2)-3}$_3$)$_2$], though the pyrazolyl ring substituents dramatically affect the behavior of the ligand.[16]

The ^{1}H NMR spectrum of complex **5** confirms that the ratio of Re/Ag/CH(C$_3$H$_3$N$_2$-1)$_3$ is 2:2:1 in solution. Even when a 2-fold excess of CH(C$_3$H$_3$N$_2$-1)$_3$ was used, product **5** was always isolated upon workup. The ^{1}H NMR spectrum at 25 °C displays two doublets at δ 7.85 and 7.94 for the H^{3,5} protons (Table 2), each of which is coupled to a central H^4 proton which gives rise to a doublet-of-doublets at δ 6.60 (J(HH) = 2 and 2 Hz). This is clearly not representative of the solid-state structure, as it suggests all three pyrazolyl rings are equivalent in solution. A ^{1}H NMR spectrum measured at −80 °C in CD$_2$Cl$_2$ revealed a modicum of broadening of the resonances at δ 7.85 and 7.94, though neither coalescence nor could the low-temperature limiting spectrum be attained. At ambient temperatures the scrambling of the silver atoms about the polyhedral rhenacarborane cages must be accompanied by rapid exchange of the coordinating pyrazolyl ring nitrogen atoms between the silver centers themselves. Slight thermal suppression of this latter process might account for the observed broadening in the ^{1}H NMR spectrum at −80 °C.

Using another excellent chelating ligand for silver(I), 2,2′-dipyridyl, the complex [ReAg(μ-10-H-η^5-7,8-C$_2$B$_9$H$_{10}$)(CO)$_3${κ^2-(C$_5$H$_4$N-2)$_2$}] (**6**) was isolated from the reaction between the salt **1** and a 1:1 mixture of Ag[BF$_4$] and (C$_5$H$_4$N-2)$_2$. The IR spectrum of complex **6** displayed the usual three CO absorptions at 2018, 1933, and 1917 cm^{-1} expected for adduct formation between the anion of salt **1** and a cationic silver(I) fragment. The ^{1}H and ^{13}C{^{1}H} NMR spectra (Table 2) showed a typical pattern for a coordinated 2,2′-dipyridyl ligand in a mirror or pseudomirror symmetric environment. The *endo*-Re(CO)$_3$ carbonyl-carbon nuclei resonate in the latter spectrum at δ 192.7, the observation of one peak once again due to the inevitable dynamic behavior in solution. An X-ray structure determination was not possible and so to confirm the 1:1:1 Re/Ag/2,2′-dipyridyl ratio FAB mass spectra were measured. Indeed in the positive ion FAB mass spectrum a peak maximum was observed at m/z 667.1 (ca. 100% rel height, calcd (**6**$^+$) 668.1) with an isotope envelope closely matching that of the calculated spectrum. A smaller cluster of peaks (max. m/z 931.2, rel height 37%) was also seen and corresponds to a molecular ion [**6** + Ag{(C$_5$H$_4$N-2)$_2$}]$^+$ (calcd 930.8). It was intriguing to examine whether the latter species could be observed in solution under ambient conditions. There was no evidence of it in the NMR spectra of **6**, nor was there any suggestion of its existence when the salt **1** was treated with 2 mol equiv each of Ag[BF$_4$] and 2,2′-dipyridyl. Thus it seems that this supermolecular ion is formed under the conditions of the FAB mass spectrum experiment. A negative ion FAB mass spectrum revealed the presence, as expected, of the anion of **1** (max. m/z 403.6, calcd 402.7). In the absence of an X-ray structural study, it is nevertheless believed that in the solid state the 2,2′-dipyridyl ligand in **6** adopts a similar lopsided disposition to that of CH$_2$(C$_3$H$_3$N$_2$-1)$_2$ in complex **4**.

Chart 2

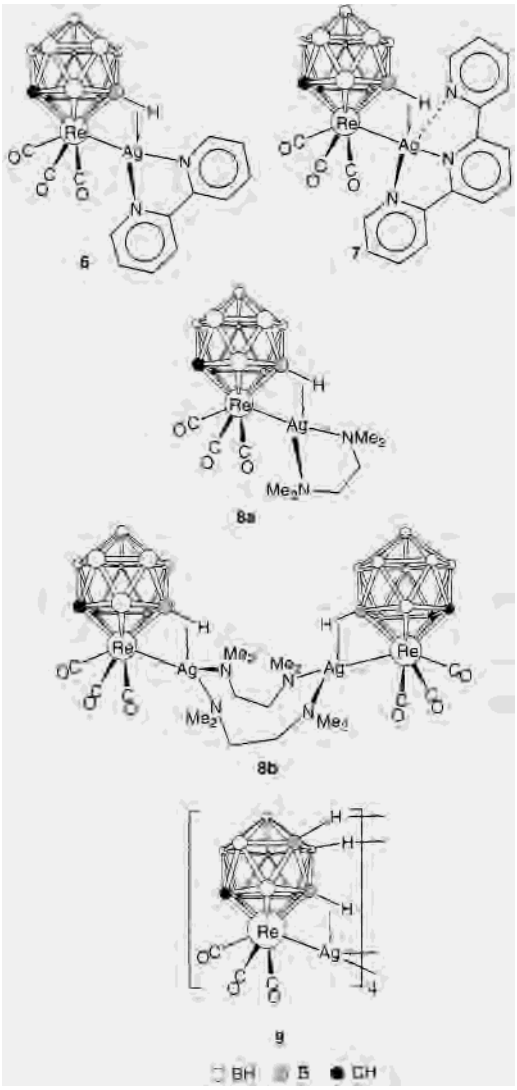

As a logical extension to this work, and as an alternative probe for structural elucidation, the salt **1** was treated with a 1:1 mixture of Ag[BF$_4$] and 2,2′:6′,2″-terpyridyl. This time X-ray quality crystals of the product [ReAg(μ-10-H-η^5-7,8-C$_2$B$_9$H$_{10}$)(CO)$_3${κ^3-C$_5$H$_3$N(C$_5$H$_4$N-2)$_2$-2,6}] (**7**) were successfully grown. The results of an X-ray structural study are given in Table 6, and the molecule is shown in Figure 5. It is composed of the basic Re−β-B−H⇀Ag core with the Re−Ag (3.0295(6) Å) connectivity somewhat longer than observed in the structures of **2** (2.9344(12)),[8a] **3** (2.9457(6)), **4** (2.8825(7)), and **5** (av. 2.9020 Å). The Ag−B(4) distance in complex **7** (2.560(7) Å) is also marginally longer than the corresponding distances in **2** (2.449(14)),[8a] **3** (2.442(6)), **4** 2.507(6)), and **5** (av 2.481 Å). The coordination sphere around the silver atom is completed by the κ^3-2,2′:6′,2″-terpyridyl ligand to give a highly unusual pentacoordinated silver(I) center, assuming the rhenium atom and β-B−H bond each occupy one site. The binding of the terpyridyl ligand is not surprisingly asymmetric with respect to the Re−Ag−B(4) mean plane such that the central nitrogen (Ag−N(31) 2.361(5) Å) is displaced by ca. 0.6 Å from said plane. The nitrogen atoms N(21) and N(41) of the two distal rings are situated at distances of 2.568(5) and 2.365(5) Å from the silver, respectively, and deviate by ca. 2.4 and 1.9 Å from either side of the Re−Ag−B(4) mean plane. The Ag−N bond

(15) (a) Harlow, R. L.; Thompson, J. S.; Whitney, J. F. *J. Am. Chem. Soc*. **1983**, *105*, 3522. (b) Carrier, S. M.; Houser, R. P.; Ruggiero, C. E.; Tolman, W. B. *Inorg. Chem*. **1993**, *32*, 4889. (c) Chen, J.-D.; Lee, C.-T.; Liou, L.-S.; Wang, J.-C. *Inorg. Chim. Acta* **1996**, *249*, 115.

(16) Humphrey, E. R.; Harden, N. C.; Rees, L. H.; Jeffery, J. C.; McCleverty, J. A.; Ward, M. D. *J. Chem. Soc., Dalton Trans*. **1998**, 3353 and references therein.

Table 6. Selected Internuclear Distances (Å) and Angles (deg) for [ReAg(μ-10-H-η^5-7,8-$C_2B_9H_{10}$)(CO)$_3$\{κ^3-$C_5H_3N(C_5H_4N$-2)$_2$-2,6\}] (**7**)

Re−C(5)	1.902(8)	Re−C(3)	1.909(8)	Re−C(4)	1.917(7)	Re−C(2)	2.295(6)
Re−C(1)	2.299(6)	Re−B(3)	2.356(7)	Re−B(5)	2.358(7)	Re−B(4)	2.393(6)
Re−Ag	3.0295(6)	B(4)−H(4)	1.15(6)	B(4)−Ag	2.560(7)	C(3)−O(3)	1.157(9)
C(4)−O(4)	1.141(10)	C(5)−O(5)	1.161(10)	Ag−H(4)	1.86(6)	Ag−N(31)	2.361(5)
Ag−N(41)	2.365(5)	Ag−N(21)	2.568(5)				

C(5)−Re−C(3)	92.5(4)	C(5)−Re−C(4)	85.0(3)	C(5)−Re−Ag	73.4(2)
C(3)−Re−Ag	64.7(2)	C(4)−Re−Ag	141.9(2)	B(4)−Re−Ag	54.8(2)
Re−B(4)−Ag	75.3(2)	O(3)−C(3)−Re	176.0(9)	O(4)−C(4)−Re	178.2(7)
N(31)−Ag−N(41)	69.8(2)	N(31)−Ag−B(4)	162.1(2)	N(41)−Ag−B(4)	125.0(2)
N(31)−Ag−N(21)	66.4(2)	N(41)−Ag−N(21)	134.0(2)	B(4)−Ag−N(21)	96.5(2)
N(31)−Ag−Re	138.29(12)	N(41)−Ag−Re	113.68(13)	B(4)−Ag−Re	49.8(2)
N(21)−Ag−Re	108.05(14)				

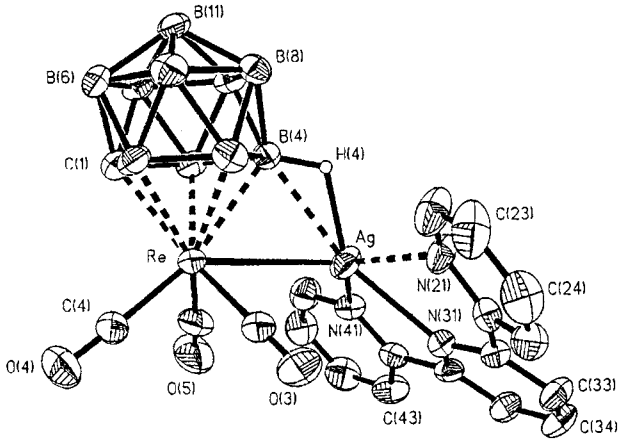

Figure 5. Structure of [ReAg(μ-10-H-η^5-7,8-$C_2B_9H_{10}$)(CO)$_3$\{κ^3-C_5H_3N-(C_5H_4N-2)$_2$-2,6\}] (**7**), showing the crystallographic labeling scheme. Thermal ellipsoids are shown at the 40% probability level. Only the agostic hydrogen atom is shown for clarity.

lengths are comparable or considerably less than the corresponding distances for the κ^3-2,2′:6′,2″-terpyridyl ligand in the complex [Ag(PPh$_3$)\{κ^3-$C_5H_3N(C_5H_4N$-2)$_2$-2,6\}][ClO$_4$] (Ag−N(central) 2.457(2) and Ag−N(distal) 2.561(2) and 2.614(2) Å)[17] so that we can confidently describe the bonding of the tricyclic ligand in **7** as tridentate κ^3, albeit in an asymmetric manner. The Re−Ag−B(4) and Ag−N(21)−N(31)−N(41) mean planes are subtended at an angle of 100.5° and are thus perpendicular to one another, resulting in a distorted trigonal−bipyramidal coordination geometry for the silver, with the axial N(21) and N(41) atoms bent toward one another (N(21)−Ag-N(41) 134.0(2)°). This is very similar in magnitude to that in [Ag(PPh$_3$)\{κ^3-$C_5H_3N(C_5H_4N$-2)$_2$-2,6\}][ClO$_4$] (130.0(1)°).

The molecule is, as expected, dynamic in solution with resonances in the ^{1}H and ^{13}C\{^{1}H\} NMR spectra for the κ^3-2,2′:6′,2″-terpyridyl ligand with local pseudo C_s symmetry. Thus eight resonances are observed for this ligand in the ^{13}C\{^{1}H\} NMR spectrum (Table 2) with the C^{2,6} and C$^{2',6'}$ carbon atoms ortho to the nitrogens appearing at characteristic chemical shifts of δ 153.5, 152.2, and 151.7.

The coordination of di- and terpyridyl ligands notwithstanding, we wanted to assess the ability of a chelating diamine molecule to ligate a silver atom in our argentarhenacarborane system. The ligand of choice was $Me_2N(CH_2)_2NMe_2$ (*N*,*N*,*N*′,*N*′-tetramethylethylenediamine) which upon treatment with salt **1** and Ag[BF$_4$] gave [\{ReAg(μ-10-H-η^5-7,8-$C_2B_9H_{10}$)(CO)$_3$\}$_2$-\{μ-$Me_2N(CH_2)_2NMe_2$\}$_2$] (**8**). Adduct formation was deduced initially from the IR spectrum (ν_{max}(CO) 2018, 1934, and 1916 cm^{-1}). Because of the rapid dynamic activity of the bimetallic molecule on the NMR time scale (as deduced by low-temperature NMR measurements), the NMR spectra (Table 2) afford little detailed information regarding the structure of the molecule. Compound **8** is light sensitive, extremely air sensitive, and does not yield X-ray quality crystals. Structure **8a** is a reasonable suggestion for the solid-state configuration based on the established structures of compound **4** or **6**. In a positive ion FAB mass spectrum of complex **8** a set of peaks with a maximum at *m*/*z* 627.1 was observed which does correspond to a species with the formula of **8a** (calcd 628.1), but there was little of this present (rel height 40%). A peak at higher mass (max. *m*/*z* 851.2) was observed at a much greater level (rel. height 100%) and can be attributed to a species [**8a** + Ag-\{$Me_2N(CH_2)_2NMe_2$\}$_2$]$^+$ (calcd 850.8). Such a moiety might result from the fragmentation of a tetranuclear metal complex **8b** by loss of the anion [Re(CO)$_3$(η^5-7,8-$C_2B_9H_{11}$)]$^-$, which was itself detected in significant quantity in a negative ion FAB mass spectrum of a sample of **8**. The dimer **8b** may therefore be a better representation of the solid-state structure. In solution both **8a** and **8b** are plausible contributors to the dynamic profile, and amine exchange between the silver atoms is likely to be facile.

While we have begun to address some of the options available for completing the coordination sphere of the silver atom with phosphines and nitrogen ligands, we have up to now not discussed the possibility of combining salt **1** with Ag[BF$_4$] alone. The latter has been used as a powerful oxidant of the metallacarborane anionic complexes [Mo(CO)$_3$(η^5-7,8-Me$_2$-7,8-$C_2B_9H_9$)]$^{2-}$ and [Re(CO)$_3$(η^5-7-$CB_{10}H_{11}$)]$^{2-}$, with the latter decomposing upon treatment.[18] Reaction of the salt **1** with 1 mol equiv of Ag[BF$_4$] in a 1:4 solvent mixture of THF and CH_2Cl_2 gave a white microcrystalline product [ReAg\{μ-5,6,-10-(H)$_3$-η^5-7,8-$C_2B_9H_8$\}(CO)$_3$]$_4$ (**9**) that was very soluble in THF but almost completely insoluble in neat CH_2Cl_2. This necessitated measurement of the NMR spectrum in d_8-THF. Despite this suitable solvent the NMR spectral information was limited to confirming the presence of the [Re(CO)$_3$(η^5-7,8-$C_2B_9H_{11}$)]$^-$ fragment somehow in combination with Ag$^+$ ions. This was also evident in the IR spectrum (Table 1) with ν_{max}(CO) absorptions at 2026, 1942, and 1929 cm^{-1}, in the range expected for a neutral rhenium−silver species. In solution (from −80 to −25 °C) dynamic behavior occurs probably involving polyhedral silver scrambling with THF molecules likely coordinated in some manner to the silver and exchanging rapidly.

Suitable crystals of complex **9** were fortunately isolated from a CH_2Cl_2−THF−light petroleum mixture so that an X-ray diffraction study could be carried out. Pertinent structural parameters are listed in Table 7 and the structure is shown in

(17) Ainscough, E. W.; Brodie, A. M.; Ingham, S. L.; Waters, J. M. *J. Chem. Soc., Dalton Trans.* **1994**, 215.

(18) (a) Dossett, S. J.; Li, S.; Stone, F. G. A. *J. Chem. Soc., Dalton Trans.* **1993**, 1585. (b) Blandford, I.; Jeffery, J. C.; Jelliss, P. A.; Stone, F. G. A. *Organometallics* **1998**, *17*, 1402.

Table 7. Selected Internuclear Distances (Å) and Angles (deg) for [ReAg{μ-5,6,10-(H)$_3$-η^5-7,8-$C_2B_9H_8$}(CO)$_3$]$_4$ (**9**)

Re−C(11)	1.922(6)	Re−C(12)	1.937(6)	Re−C(13)	1.939(6)	Re−C(1)	2.299(5)
Re−C(2)	2.311(5)	Re−B(3)	2.356(6)	Re−B(5)	2.370(6)	Re−B(4)	2.410(6)
Re−Ag	2.8702(6)	Re−Re[a]	6.7790(7)	Ag−B(4)	2.564(6)	Ag−B(9a)[a]	2.905(6)
Ag−B(8a)[b]	2.978(7)	Ag−H(9a)[b]	2.08(4)	Ag−H(8a)[a]	2.02(4)	Ag−Ag[a]	4.6512(9)
Ag−H(4)	1.91(4)	B(4)−H(4)	1.20(4)	B(8)−H(8)	1.09(6)	B(9)−H(9)	1.08(6)
C(11)−O(11)	1.161(7)	C(12)−O(12)	1.141(8)	C(13)−O(13)	1.146(8)		

C(11)−Re−C(12)	84.4(3)	C(11)−Re−C(13)	95.6(3)	C(12)−Re−C(13)	82.9(2)
B(4)−Re−Ag	57.3(2)	Re−B(4)−Ag	70.4(2)		

[a] Symmetry transformations used to generate equivalent atoms: $-y + 1/4, x + 1/4, -z + 1/4$. [b] Symmetry transformations used to generate equivalent atoms: $y - 1/4, -x + 1/4, -z + 1/4$.

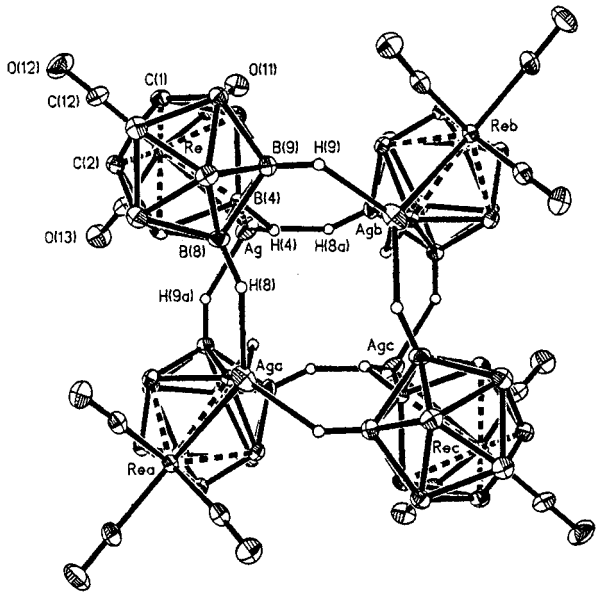

Figure 6. Structure of [ReAg{μ-5,6,10-(H)$_3$-η^5-7,8-$C_2B_9H_8$}(CO)$_3$]$_4$ (**9**), showing the crystallographic labeling scheme. Thermal ellipsoids are shown at the 40% probability level. Only the agostic hydrogen atoms are shown for clarity.

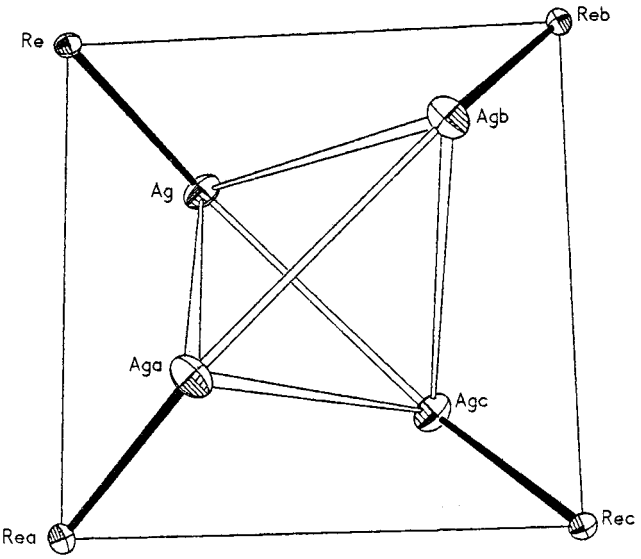

Figure 7. Arrangement of the rhenium and silver atoms in the tetrameric structure of **9**.

Figure 6. The molecule is composed of a tetrameric arrangement of four equivalent neutral [ReAg(μ-10-H-η^5-7,8-$C_2B_9H_{10}$)(CO)$_3$] units in the $I4_1/a$ space group. Within each unit the Re−Ag bond (2.8702(5) Å) is bridged by a carborane cage via the β-B−H vertex in the CCB*B*B ring (Ag−B(4) 2.564(6) Å), giving the familiar intraunit B(4)−H(4) ⇀ Ag bond. Completing the approximately tetrahedral silver ion environment are two interunit B−H ⇀ Ag interactions between the silver and the B−H vertexes of the noncoordinating B_5 rings of each of the two adjacent rhenacarborane units. The Ag−H connectivities (Ag−H(8a) 2.02(4) and Ag−H(9a) 2.08(4) Å) are quite within acceptable limits for a bridging hydrogen bound to a silver(I) center,[7,8] but the Ag−B distances are ca. 0.3−0.4 Å longer (Ag−B(8a) 2.978(7) and Ag−B(9a) 2.905(6) Å) than the intraunit Ag−B(4) contact, though ca. 0.5−0.6 Å shorter than the intermolecular Ag···B distance (3.490(9) Å) discussed for the structure of complex **3**. Thus these interunit B−H ⇀ Ag interactions appear to be intermediate between the regular covalent agostic bonding and the longer range electrostatic intermolecular attractions. The assembly of the metals in the tetramer is best appreciated from Figure 7. The rhenium atoms lie in a square which is slightly distorted from planarity and with edge lengths of 6.7790(7) Å. The silver atoms, on the other hand, sit within this square in a tetrahedral formation with edge lengths of 4.6512(9) Å.

Conclusion

A consistent feature in all the structural determinations presented is that a carborane cage bridges a Re−Ag bond utilizing the β-B−H bond from the CCB*B*B face coordinating the rhenium atom. For this particular bimetallic system, this would seem to represent the most stable ground-state configuration. Alternative *exo*−*closo* structures with no Re−Ag bonds are, however, clearly accessible in solution at ambient and even low temperatures, interchanging rapidly, and so actually impeding full scrutinisation of the dynamic behavior. Nevertheless, the solid state structures are particularly interesting from the perspectives of uncharacteristic ligand behavior (e.g., tris(pyrazol-1-yl)methane in complex **5**), unusual silver coordination number and geometry (as in complex **7**), and novel metallacarborane cluster assembly (as in complex **9**), and we anticipate further strides to be made in this area of metallacarborane chemistry.

Experimental Section

General Considerations. All experiments were conducted under an atmosphere of dry nitrogen using Schlenk tube techniques. Solvents were freshly distilled under nitrogen from the appropriate drying agents before use. Light petroleum refers to that fraction of boiling point 40−60 °C. Celite and silica gel (Acros, 60−200 mesh) pads for filtration were ca. 4 cm thick. The NMR measurements were recorded at the following frequencies: ^{1}H at 360.13, ^{13}C at 90.56, ^{11}B at 115.55, and ^{31}P at 145.78 MHz. The reagents **1**,[8a] bis(pyrazol-1-yl)methane, and tris(pyrazol-1-yl)methane[19] were made as described previously. The compounds Ag[BF_4], 1,2-bis(diphenylphosphino)ethane, 2,2′-dipyridyl, 2,2′:6′,2″-terpyridyl, and *N*,*N*,*N*′,*N*′-tetramethylethylenediamine were purchased from Aldrich.

[{ReAg(μ-10-H-η^5-7,8-$C_2B_9H_{10}$)(CO)$_3$}$_2${μ-$Ph_2P(CH_2)_2PPh_2$}] (3). THF (15 mL) was added to the compounds **1** (0.17 g, 0.32 mmol),

(19) Trofimenko, S. *J. Am. Chem. Soc.* **1979**, *92*, 5118.

Table 8. Data for X-ray Crystal Structure Analyses

	3	**4**	**5**	**7**	**9**
formula	$C_{18}H_{23}AgB_9O_3P$-Re·$0.75CH_2Cl_2$	$C_{12}H_{19}AgB_9$-N_4O_3Re	$C_{20}H_{32}Ag_2B_{18}N_6$-$O_6Re_2$·$CH_2Cl_2$	$C_{20}H_{22}AgB_9N_3O_3$-Re·$0.5CH_2Cl_2$	$C_5H_{11}AgB_9O_3$-Re·$0.5C_5H_{12}$
fw	773.39	658.67	1320.16	786.23	546.57
cryst dimens (mm)	0.40 × 0.34 × 0.14	0.40 × 0.40 × 0.25	0.50 × 0.50 × 0.10	0.66 × 0.62 × 0.49	0.40 × 0.10 × 0.10
cryst color, shape	colorless parallelepiped	colorless prism	colorless prism	colorless prisms	colorless needles
cryst system	monoclinic	triclinic	monoclinic	monoclinic	tetragonal
space group	*C*2/*c*	$P\bar{1}$	*C*2/*c*	*C*2/*c*	$I4_1/a$
a(Å)	21.120(3)	7.0107(6)	39.326(7)	18.054(7)	25.746(3)
b(Å)	11.594(2)	12.431(3)	10.5952(14)	12.3798(12)	25.746(3)
c(Å)	22.926(3)	12.583(2)	21.378(3)	25.173(4)	8.6695(9)
α(deg)		83.311(14)			
β(deg)	94.078(10)	77.73(2)	114.572(13)	102.81(2)	
γ(deg)		83.60(2)			
V(Å^3)	5599.7(14)	1060.0(3)	8101(2)	5486(2)	5746.5(10)
Z	8	2	8	8	16
d_{calc}(g cm^{-3})	1.835	2.064	2.165	1.904	2.527
μ(Mo Kα)(mm^{-1})	5.240	6.650	7.088	5.250	9.777
T(K)	173(2)	293(2)	173(2)	293(2)	173(2)
2*θ* range (deg)	3.8−50.0	3.4−50.0	3.8−55.0	3.4−50.0	3.2−55.0
reflcns collcd	9007	4056	40370	4964	18035
indept reflcns	4440	3721	9211	4799	3293
R_{int}	0.0236	0.0161	0.0426	0.0415	0.0363
*wR*2 (all data), *R*1[a]	0.0633, 0.0260	0.0643, 0.0256	0.0846, 0.0321	0.0999, 0.0376	0.0812, 0.0313
weighting factors *a*, *b*[a]	0.0350, 0.0	0.0435, 0.0143	0.0532, 39.1872	0.0614, 8.7130	0.0433, 40.0345
largest diff peak and hole (e Å^{-3})	1.755, −0.639	1.049, −1.101	1.387, −2.023	1.679, −1.834	1.770, −1.920

[a] Refinement was block full-matrix least-squares on all F^2 data: $wR2 = [\sum\{w(F_o^2 - F_c^2)^2\}/\sum w(F_o^2)^2]^{1/2}$ where $w^{-1} = [\sigma^2(F_o^2) + (aP)^2 + bP]$ where $P = [\max(F_o^2,0) + 2F_c^2]/3$. The value $R1 = \sum||F_o| - |F_c||/\sum|F_o|$ with $F_o > 4\sigma(F_o)$ and $w^{-1} = [\sigma^2(F_o) + g(F_o^2)]$.

$Ag[BF_4]$ (0.06 g, 0.31 mmol), and 1,2-bis(diphenylphosphino)ethane (0.06 g, 0.15 mmol) and the resulting suspension stirred for 1 h. Solvent was removed in vacuo and CH_2Cl_2−light petroleum (5 mL, 4:1) added. The suspension, comprising an off-white precipitate in a colorless solution, was filtered though a short silica plug. Solvent was removed in vacuo and the residue crystallized from CH_2Cl_2−light petroleum (10 mL, 1:1) to yield white microcrystals of [{ReAg(*μ*-10-H-η^5-7,8-$C_2B_9H_{10}$)$(CO)_3$}$_2${*μ*-$Ph_2P(CH_2)_2PPh_2$}] (**3**) (0.12 g). X-ray quality colorless crystals were grown from a CH_2Cl_2 solution layered with light petroleum.

[ReAg(*μ*-10-H-η^5-7,8-$C_2B_9H_{10}$)$(CO)_3${κ^2-$CH_2(C_3H_3N_2$-1)$_2$}] (4). Using a similar procedure (filtration using CH_2Cl_2−light petroleum (3:2)), the compounds **1** (0.10 g, 0.19 mmol), $Ag[BF_4]$ (0.04 g, 0.20 mmol) and bis(pyrazol-1-yl)methane (0.03 g, 0.20 mmol) gave white microcrystals of [ReAg(*μ*-10-H-η^5-7,8-$C_2B_9H_{10}$)$(CO)_3${κ^2-$CH_2(C_3H_3N_2$-1)$_2$}] (**4**) (0.08 g). X-ray quality colorless crystals were grown from a CH_2Cl_2 solution layered with light petroleum.

[{ReAg(*μ*-10-H-η^5-7,8-$C_2B_9H_{10}$)$(CO)_3$}$_2${*μ*-κ^1,κ^2-$CH(C_3H_3N_2$-1)$_3$}] (5). Using a similar method compound **1** (0.10 g, 0.19 mmol), $Ag[BF_4]$ (0.04 g, 0.20 mmol), and tris(pyrazol-1-yl)methane (0.02 g, 0.09 mmol) gave white microcrystals of [{ReAg(*μ*-10-H-η^5-7,8-$C_2B_9H_{10}$)$(CO)_3$}$_2${*μ*-κ^1,κ^2-$CH(C_3H_3N_2$-1)$_3$}] (**5**) (0.16 g). X-ray quality colorless crystals were grown from a CH_2Cl_2 solution layered with light petroleum.

[ReAg(*μ*-10-H-η^5-7,8-$C_2B_9H_{10}$)$(CO)_3${κ^2-(C_5H_4N-2)$_2$}] (6). The same procedure with compound **1** (0.16 g, 0.31 mmol), $Ag[BF_4]$ (0.06 g, 0.31 mmol), and 2,2′-dipyridyl (0.06 g, 0.38 mmol) gave white microcrystals of [ReAg(*μ*-10-H-η^5-7,8-$C_2B_9H_{10}$)$(CO)_3${κ^2-(C_5H_4N-2)$_2$}] (**6**) (0.16 g) crystallized from CH_2Cl_2−light petroleum (10 mL, 1:1).

[ReAg(*μ*-10-H-η^5-7,8-$C_2B_9H_{10}$)$(CO)_3${κ^3-C_5H_3N(C_5H_4N-2)$_2$-2,6}] (7). Similarly, white microcrystals of [ReAg(*μ*-10-H-η^5-7,8-$C_2B_9H_{10}$)-$(CO)_3${κ^3-C_5H_3N(C_5H_4N-2)$_2$-2,6}] (**7**) (0.12 g) were obtained from compound **1** (0.10 g, 0.19 mmol), $Ag[BF_4]$ (0.04 g, 0.20 mmol), and 2,2′:6′,2″-terpyridyl (0.05 g, 0.21 mmol).

[{ReAg(*μ*-10-H-η^5-7,8-$C_2B_9H_{10}$)$(CO)_3$}$_2${*μ*-$Me_2N(CH_2)_2NMe_2$}$_2$] (8). The compounds **1** (0.12 g, 0.22 mmol) and $Ag[BF_4]$ (0.04 g, 0.21 mmol) were dissolved in THF (15 mL) and cooled to −80 °C. A solution of *N*,*N*,*N*′,*N*′-tetramethylethylenediamine (35 *μ*L, 0.23 mmol) in THF (5 mL) was added via a dropping funnel. The mixture was warmed to room temperature while stirring. Solvent was removed in vacuo and CH_2Cl_2 (15 mL) added to give a suspension which was filtered through Celite. The filtrate was reduced in volume in vacuo to ca. 2 mL and Et_2O (10 mL) carefully added to produce a fine off-white precipitate. This was allowed to settle and the supernatant withdrawn into a 20 mL syringe via a 0.45 *μ*m puradisc filter. The clear solution was transferred to another Schlenk tube, and solvent was removed in vacuo. Off-white microcrystals of [{ReAg(*μ*-10-H-η^5-7,8-$C_2B_9H_{10}$)$(CO)_3$}$_2${*μ*-$Me_2N(CH_2)_2NMe_2$}$_2$] (**8**) (0.04 g) were formed by crystallization from CH_2Cl_2−light petroleum (10 mL, 1:4).

[ReAg{*μ*-5,6,10-$(H)_3$-η^5-7,8-$C_2B_9H_8$}$(CO)_3]_4$ (9). The compounds **1** (0.20 g, 0.37 mmol) and $Ag[BF_4]$ (0.08 g, 0.41 mmol) were dissolved in THF−CH_2Cl_2 (10 mL, 1:4) and stirred for 1 h, during which time a pale precipitate of $Cs[BF_4]$ formed. The solution was filtered through Celite. The filtrate was reduced in volume in vacuo to ca. 2 mL and light petroleum (8 mL) added to give a white precipitate of [ReAg{*μ*-5,6,10-$(H)_3$-η^5-7,8-$C_2B_9H_8$}$(CO)_3]_4$ (**9**) (0.14 g). X-ray quality colorless crystals were grown from a THF−CH_2Cl_2−light petroleum (1:4:5) mixture at −20 °C.

Structure Determinations of Compounds 3, 5, and 9. Complexes **3** and **5** crystallize with 0.75 and 1 molecule, respectively, of CH_2Cl_2 in the asymmetric unit, while **9** does so with 0.5 molecule of pentane. All crystals were mounted on glass fibers, and low-temperature data were collected on a Siemens SMART CCD area-detector three-circle diffractometer (Mo Kα X-radiation, graphite monochromator, $\bar{\lambda}$ = 0.71073 Å). For three or four settings of *φ*, narrow data "frames" were collected for 0.3° increments in *ω*. For each of the complexes **3** and **9** just over a hemisphere of data was collected while for the crystal of **5** a full sphere of data was collected. It was confirmed that crystal decay had not taken place during the course of the data collections. The substantial redundancy in data allows empirical absorption corrections (SADABS[20]) to be applied using multiple measurements of equivalent reflections. The data frames were integrated using SAINT.[20]

Structures were solved by conventional direct methods and refined by full-matrix least-squares on all F^2 data using Siemens SHELXTL version 5.03 or SHELXL-97.[20] For both structures the non-hydrogen atoms were refined with anisotropic thermal parameters with the exception of those in the solvent molecule in **3**. The agostic B−H ⇀ Ag hydrogen atoms H(4) in complex **3**, H(104) and H(204) in **5**, and

(20) Siemens X-ray Instruments, Madison, WI, 1997.

H(4), H(8), and H(9) in complex **9** were located from final difference Fourier syntheses, and their positions were refined, some with restraints. The isotropic thermal parameters of H(8) and H(9) in **9** were also refined. All other hydrogen atoms were included in calculated positions and allowed to ride on the parent boron or carbon atoms with isotropic thermal parameters ($U_{iso} = 1.2 \times U_{iso}$ of the parent atom). The CH_2Cl_2 molecules in **3** and **5** were disordered and the pentane molecule in **9**, which is centered on a special position, was not assigned any hydrogen atoms. All calculations were carried out on Silicon Graphics Iris, Indigo, or Indy computers, and the experimental data are summarized in Table 8.

Structure Determinations of Compounds 4 and 7. Crystals of **7** grew with half a molecule of CH_2Cl_2 in the asymmetric unit. Diffracted intensities were collected on an Enraf-Nonius CAD-4 operating in the $\omega-2\theta$ (**4**) or $\omega-4/3\theta$ (**7**) scan modes, using graphite-monochromated Mo Kα X-radiation ($\bar{\lambda} = 0.71073$ Å). For each structure, the final unit cell dimensions were determined from the setting angle values of 25 accurately centered reflections. The stability of the crystals during the period of the data collections was monitored by measuring the intensities of three standard reflections every 2 h. The data were corrected for Lorentz, polarization, and X-ray absorption effects, the latter using either a numerical method based on the mesurements of crystal faces (**7**) or a semiempirical method (**4**) based on azimuthal scans of Ψ-data.

Structures were solved by direct methods and successive Fourier difference syntheses were used to locate all non-hydrogen atoms, using the SHELXTL-PC package.[20] Refinements were made by full-matrix least-squares on F^2 data, using SHELXL-97,[20] with anisotropic thermal parameters for all non-hydrogen atoms. The agostic B−H ⇀ Ag hydrogen atoms H(4) in **4** and **7** were located in final difference Fourier syntheses, their coordinates freely refined and isotropic thermal parameters fixed. All other hydrogen atoms were included in calculated positions and allowed to ride on their parent boron or carbon atoms with fixed isotropic thermal parameters ($U_{iso} = 1.2 \times U_{iso}$ of the parent atom). The solvent molecule in **7** was disordered. Atomic scattering factors were taken from the usual source.[21] All calculations were carried out on Dell PC computers, and the experimental data are summarized in Table 8.

Acknowledgment. We thank the Robert A. Welch Foundation for support (Grant AA-1201).

Supporting Information Available: Tables of atomic coordinates and *U* values, bond lengths and angles, and anisotropic thermal parameters and ORTEP diagrams for **3**, **4**, **5**, **7**, and **9** in CIF format. This material is available free of charge via the Internet at http://pubs.acs.org.

IC001140C

(21) *International Tables for X-ray Crystallography*; Kynoch Press: Birmingham, U.K.; 1974, Vol. 4.